CHEMISTRY
A EUROPEAN JOURNAL

DOI: 10.1002/chem.201002865

Hydroxydialkylamino Cruciforms: Amphoteric Materials with Unique Photophysical Properties

Psaras L. McGrier,[b] Kyril M. Solntsev,[b] Anthony J. Zucchero,[b] Oscar R. Miranda,[c] Vincent M. Rotello,[c] Laren M. Tolbert,[b] and Uwe H. F. Bunz*[a, b]

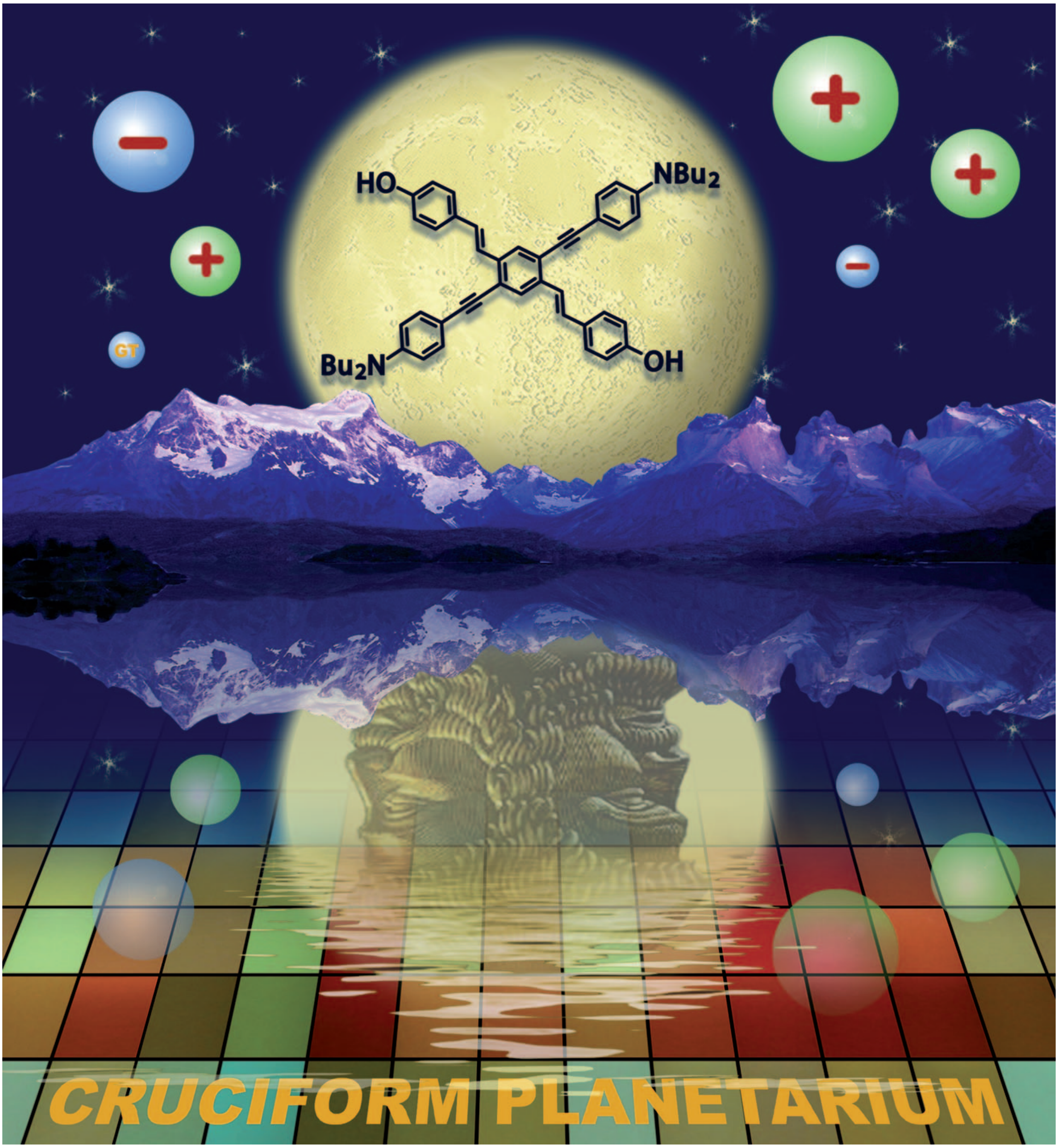

WILEY ONLINE LIBRARY

Abstract: Two amphoteric cruciforms **6** and **7** (XF; 4,4′-[(1*E*,1′*E*)-(2,5-bis{[4-(dibutylamino)phenyl]ethynyl}-1,4-phenylene)bis(ethene-2,1-diyl)]diphenol, 4,4′-[{2,5-bis[(*E*)-4-(dibutylamino)styryl]-1,4-phenylene}bis(ethyne-2,1-diyl)]-diphenol) were prepared by a Horner reaction followed by a Sonogashira coupling and subsequent deprotection. The XFs display significant changes in absorption and emission when exposed to trifluoroacetic acid, tetrabutylammonium hydroxide, and metal triflates. The substitution pattern of **6** and **7** leads to spatial separation of the frontier molecular orbitals, which allows the HOMO or LUMO of the XF to be addressed independently by acidic or basic agents. XF **6**, which has hydroxyl groups on the styryl axis, displays changes in emission color upon exposure to ten amines in eight different solvents. The change in fluorescence upon the addition of amines was analyzed by linear discriminant analysis. These XFs may have potential in sensor applications for metal cations and amines.

Keywords: alkynes • amines • fluorescence • sensors • solvatochromism

Introduction

1,4-Distyryl-2,5-bis(arylethynyl)benzenes (cruciforms, XFs) containing basic nitrogens, pyridines, phenols, and phenothiazines as functional appendages are known.[1] Herein we have prepared an XF-based fluorescence probe (**6**) that is sensitive to both cationic/acidic and basic agents and is potentially useful as a dual function sensor.

The spectroscopic behavior of amphoteric photoacids/photobases can be complicated by multiple acid–base equilibria between different species in the ground state, including the formation of zwitterions. However, a more serious drawback for such materials can result from their excited-state dynamics because they may undergo phototautomerization when the two functions are not vicinal. Protons can be shuttled along hydrogen-bond wires formed in protic solvents[2] as the result of a potentially dramatic increase in the acidity or basicity of the corresponding functional groups upon excitation.[2a,3,4]

An attractive way to simplify the prototropic behavior of chromophores in the ground and excited states and to prevent tautomerization is to separate the acidic and basic moieties spatially and electronically. XFs with styryl and arylethynyl branches attached to a central benzene ring allow the spatial separation of the frontier molecular orbitals (FMOs) upon suitable donor–acceptor substitution of the peripheral aryl units.[1] Similar examples of such disjointed FMO structures include Haley's 1,2,4,5-tetrakis(arylethynyl)benzenes,[5] Scherf's swivel cruciforms,[6] Diederich's tetraethynylethylenes,[7] and Galvin's distyrylbenzene derivatives.[8] By placing hydroxyl and amino groups on different axes of the XFs, as in **6** and **7**, we hope to generate spectral responses upon the addition of various acid–base analytes.

If pyridines or dialkylanilines are incorporated into the π system of the XF, either a red or blue color change in emission is observed upon coordination to metal cations. When both functional groups are present, a two-stage metalloresponsive fluorophore results.[9] With hydroxyl groups, spectroscopic changes (redshift in absorption and emission) are observed upon deprotonation, an effect which is useful for the identification of amines.[10] Herein we incorporate dialkylaniline and hydroxyl substituents into one XF to study the photophysics of amphoteric compounds by creating a two-stage probe that is responsive to protons, metal cations, bases, and amines.

Results and Discussion

Synthesis of hydroxydialkylamino XFs: The synthesis of XFs **6** and **7** started with a Horner[11] reaction of **2a** or **2b** to give distyrylbenzene derivatives **3a** and **3b** in 77 and 71 % yield, respectively, after recrystallization (Scheme 1).[9,10] Subsequently, a Sonogashira coupling[12] with either **4** or **5** gave intermediates that were deprotected at −78 °C by trifluoroacetic acid (TFA) to afford XFs **6** and **7** in 84 and 82 % yield, respectively.

Spectroscopic properties of hydroxydialkylamino XFs: Figure 1 shows the absorption and emission spectra of XFs **6** and **7** in four representative solvents. The absorbance spectrum of **6** displays broad absorption maxima ranging from $\lambda = 359$ to 372 nm. XF **7** exhibits a significant charge-transfer band in all solvents at around $\lambda = 423$ to 445 nm and a single more intense absorption at $\lambda \approx 338$ nm. The absorbance

---

[a] Prof. U. H. F. Bunz
Organisch-Chemisches Institut
Ruprecht-Karls-Universität
Im Neuenheimer Feld 270, 69120 Heidelberg (Germany)
Fax: (+49) 6221548404
E-mail: uwe.bunz@oci.uni-heidelberg.de

[b] Dr. P. L. McGrier, Dr. K. M. Solntsev, Dr. A. J. Zucchero,
Prof. L. M. Tolbert, Prof. U. H. F. Bunz
School of Chemistry and Biochemistry
Georgia Institute of Technology
901 Atlantic Drive, Atlanta, GA 30332 (USA)

[c] O. R. Miranda, Prof. V. M. Rotello
Department of Chemistry
710 North Pleasant St., University of Massachusetts Amherst
MA 01003 (USA)

Supporting information for this article is available on the WWW under http://dx.doi.org/10.1002/chem.201002865.

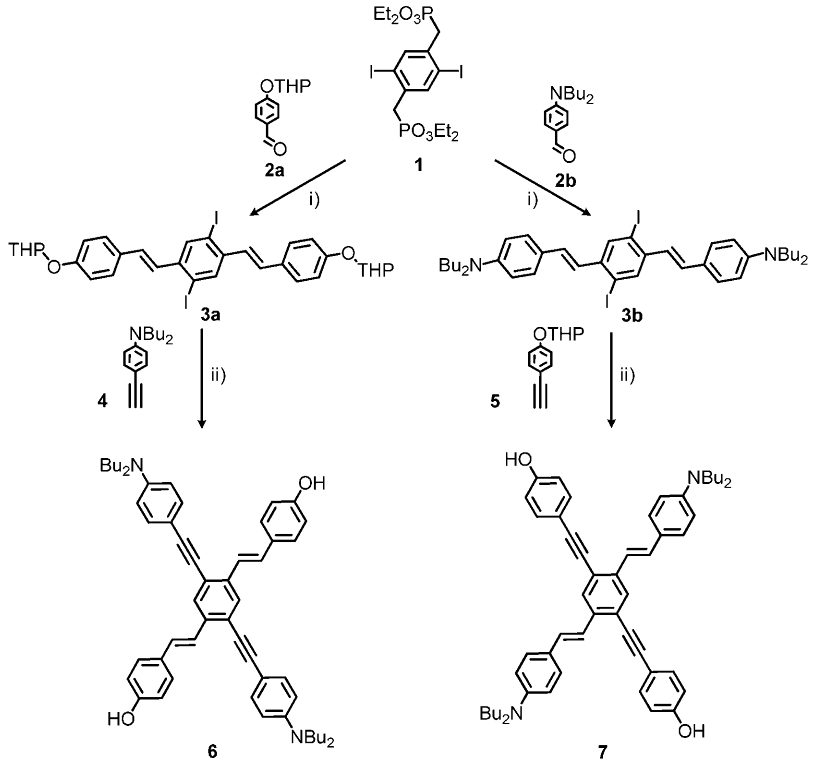

Scheme 1. Synthesis of the XFs **6** and **7**. OTHP = tetrahydropyranyl. Conditions: i) NaH, THF; ii) [$PdCl_2(Ph_3P)_2$], CuI/THF, piperidine, 25 °C then TFA, CH_2Cl_2, −78 °C.

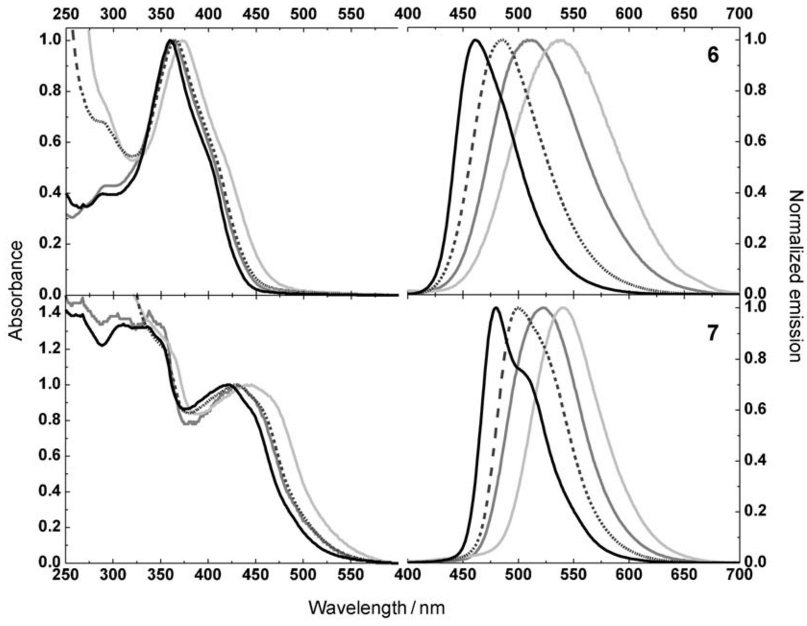

Figure 1. Absorption (left) and emission (right) spectra of **6** and **7** in diethyl ether (——), THF (-----), MeOH (——), and DMSO (——).

spectra for both compounds depend weakly on solvent polarity indicating a small ground-state dipole moment.

The emission spectra of the XFs range from $\lambda = 461$ to 540 nm (see Tables 1 and 2). XF **7** displays vibronic progressions (990 and 1180 cm^{-1}) when investigated in diethyl ether or toluene. To analyze the solvatochromic behavior of XFs **6** and **7** in emission, we used the Kamlet–Taft multivariate approach,[13] which correlates the spectral shift ν of the XF with the solvent parameters that are responsible for its acidic (α), basic (β), and polar solvating (π^*) properties.[14,15,10b] It allows a straightforward separation of selective (hydrogen bonding) and non-selective (dipole–dipole interaction) solvation.

$$\nu(1000\,\mathrm{cm}) = \nu_0 + p\pi^* + a\alpha + b\beta \tag{1}$$

The solvatochromic behavior of XFs **6** and **7** is governed by the polar and acid–base properties of the solvents (Table 3); *a*, *b*, and *p* are fitted parameters. The index π^* denotes the ability of a solvent to stabilize dipole or internal charge transfer, whereas α and β reflect the acidity and basicity of the corresponding solvent. The component *p* dominates the solvatochromic behavior of **6** and **7**, but both acidity and basicity of the solvent also induce smaller bathochromic shifts. The exception is the anion of **6**, which is formed upon reaction of **6** with diethylamine. In this case the *a* parameter is +0.8, that is, the emission is blueshifted on increasing the acidity of the solvent, whereas in the neutral and cationic species a small redshift is observed on increasing the basicity or acidity of the solvent. The large positive *a* value for the conjugate base of **6** would be expected as increasing interaction of the phenolate with a good proton donor would lead to a blueshift in the optical features through increasing neutralization of the anion by hydrogen bonding. The fluorescence quantum yield Φ in MeOH was ≈14 % for **6** and **7**. The fluorescence decays in MeOH ($\lambda = 550$ nm excitation) was 5.6 ns for **6**

Table 1. Absorption and emission maxima for **6** in various solvents.

Solvent	$\lambda_{max,abs}$ [nm]	$\lambda_{max,em}$ [nm]	Stokes shift [cm^{-1}]
MeOH	363	508	7860
MeCN	364	537	8850
DMF	369	521	7910
DMSO	372	538	8290
THF	364	485	6850
CH_2Cl_2	364	501	7510
diethyl ether	359	461	6160
toluene	363	464	6000

Table 2. Absorption and emission maxima for **7** in various solvents.

Solvent	$\lambda_{max,abs}$ [nm]	$\lambda_{max,em}$ [nm]	Stokes shift [cm^{-1}]	Vibronic progression [cm^{-1}]
MeOH	339, 431	523	10400, 4080	–
MeCN	340, 440	535	10700, 4040	–
DMF	339, 434	533	10700, 4280	–
DMSO	340, 445	540	10900, 3950	–
THF	337, 430	499	9630, 3220	–
CH_2Cl_2	339, 433	517	10200, 3750	–
diethyl ether	337, 423	480, 504	8840, 2810	990
toluene	338, 433	482, 511	8840, 2350	1180

Table 3. Solvatochromic parameters [10^3 cm] used in multivariate regression fits of emission data for XFs **6** (with and without diethylamine) and **7** according to Equation (1).

Compound	ν_0	p	a	b	R[a]
6	23±0.9	−4.0±1.4	−0.5±0.8	−0.7±1.2	0.87
6+DEA[b]	19.6±0.6	−2.5±0.9	0.8±0.5	−1.0±0.8	0.90
7	22.0±0.6	−3.1±0.9	−0.6±0.9	−0.8±0.8	0.91

[a] Correlation coefficient. [b] DEA = diethylamine.

Table 4. Photophysical data of **6** and **7** in MeOH.

	$\lambda_{max,abs}$ [nm]	$\lambda_{max,em}$ [nm]	Φ_{fl}[a]	τ_{av} [ns]
6	363	508	0.14	5.6
7	339, 431	523	0.13	1.5

[a] Quantum yield.

and 1.5 ns for **7** (Table 4). The reason for this difference is unknown.

Acid–base studies and quantum chemical calculations of hydroxydialkylamino XFs: The effect of adding an excess of TFA or tetrabutylammonium hydroxide (TBA-OH) to **6** or **7** in different solvents is shown in Figures 2 and 3. The addition of acid to **6** leads to a blueshift in absorption and emission, regardless of the solvent. The addition of tetrabutylammonium hydroxide (TBA-OH) induces a red shift in both absorption and emission of **6**. The spectral responses can be easily rationalized by assuming that the HOMO is stabilized by protonation and destabilized by deprotonation. In the neutral compound (Figure 4), the HOMO and LUMO are only slightly disjointed because both the OH and the NBu_2 substituents are electron donors. Upon deprotonation, the HOMO localizes on the phenolate that contains the distyrylbenzene axis, because more electron density is now in the system. Upon addition of TFA, the NBu_2 groups are protonated and the conjugation to the π

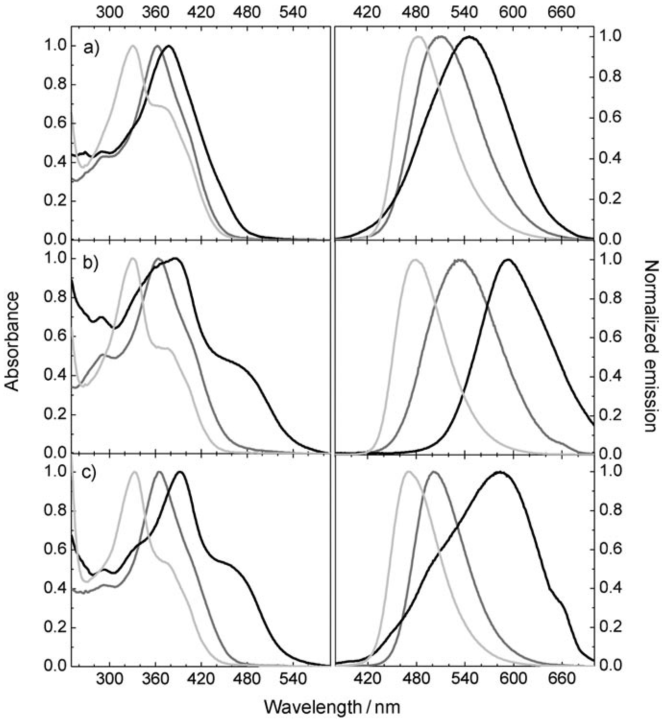

Figure 3. Absorption (left) and emission (right) spectra of **6** (——) upon addition of TFA (——) and TBA-OH (——) in a) MeOH ($\lambda_{max,abs}$ = 330 (TFA), 363 (**6**), 377 nm (TBA-OH); $\lambda_{max,em}$ = 481 (TFA), 507 (**6**), 545 nm (TBA-OH)), b) MeCN ($\lambda_{max,abs}$ = 329 (TFA), 364 (**6**), 383 nm (TBA-OH); $\lambda_{max,em}$ = 480 (TFA), 537 (**6**), 593 nm (TBA-OH)), and c) CH_2Cl_2 ($\lambda_{max,abs}$ = 332 (TFA), 364 (**6**), 391 nm (TBA-OH); $\lambda_{max,em}$ = 472 (TFA), 500 (**6**), 584 nm (TBA-OH)).

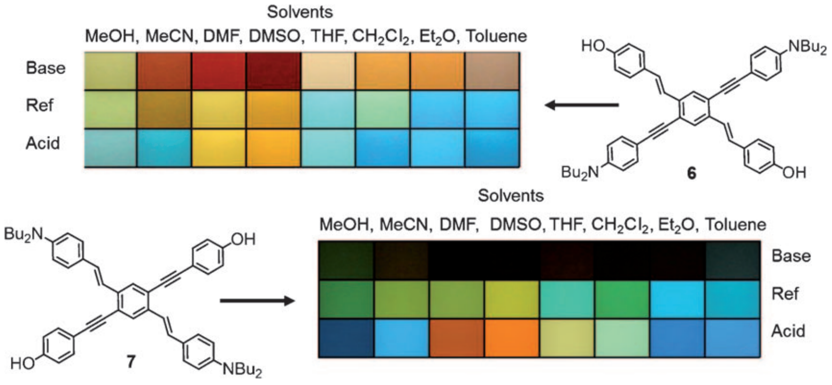

Figure 2. Exposure of **6** and **7** to trifluoroacetic acid (TFA) and tetrabutylammonium hydroxide (TBA-OH). The samples were excited by using UV radiation at λ_{em} = 366 nm.

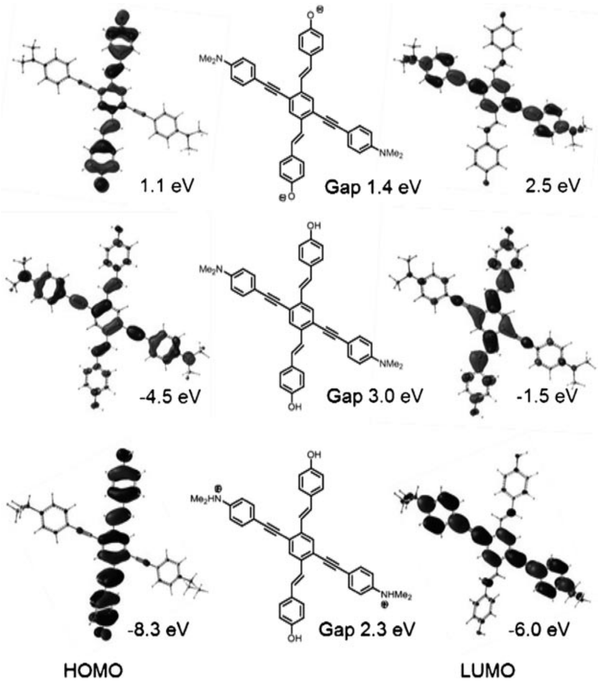

Figure 4. Molecular orbital plots of neutral (center), bisprotonated (bottom), and bisdeprotonated (top) XF **6**. The calculations were performed at the B3LYP/6-31G*//6-31G* level on a QS8-2800C-O64D QuantumCube.

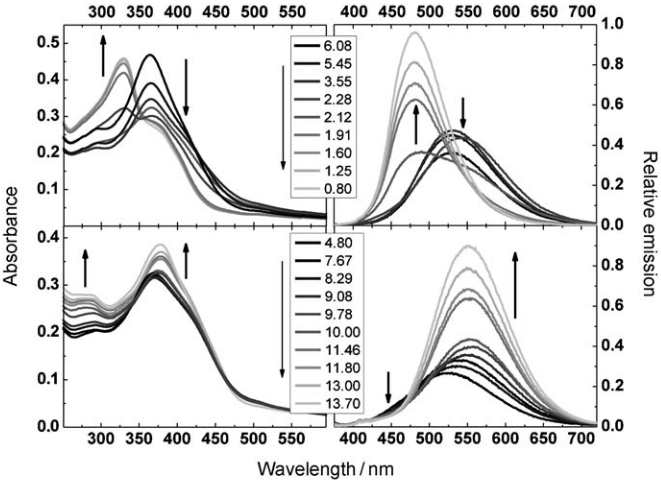

Figure 5. Absorption (left) and emission (right) spectra of **6** in MeOH/water (2:1 v/v) at different pH values. Top: Acidic titrations, bottom: basic titrations.

system is turned off. The LUMO is localized on this axis. In the protonated species, the HOMO is then localized on the (relatively) electron-rich di(hydroxystyrylbenzene) axis.

The quantum chemical calculations (B3LYP/6-31G*//6-31G*) of the neutral, bisprotonated, and bisdeprotonated forms of **6** qualitatively explain the features of the observed spectroscopic changes, but fall short for the numerical values for the HOMO–LUMO gaps. Upon deprotonation, the expected decrease in the HOMO–LUMO gap is predicted, but upon double protonation the calculations incorrectly predict a decreased HOMO–LUMO gap.[17] This failure is not too surprising because DFT calculations are not very reliable when applied to ions because the effects of the solvent are not included.

In the case of **7**, deprotonation leads to full quenching of the fluorescence. The reason for the markedly different behavior of **6** and **7** is not well understood. It has a parallel in the bis(4-hydroxyarylethynyl)benzenes, which also display only weak fluorescence upon deprotonation.[16,17]

Titration studies of hydroxydialkylamino XFs: XFs **6** and **7** are insoluble in pure water at neutral pH. To investigate their acid–base behavior, we performed titrations of **6** (see Figure 5), which is somewhat soluble in a 2:1 v/v mixture MeOH/water, but not XF **7** because it is poorly soluble even under these conditions. This data might not only reflect protonation and deprotonation, but also the dissolution of aggregates. Upon protonation with aqueous hydrochloric acid (HCl), XF **6** experiences a hypsochromic shift in absorption and emission as expected. A new band emerges at $\lambda=330$ nm along with a shoulder at $\lambda\approx370$ nm. In the emission spectrum, a new distinct band emerges at pH 0.80 ($\lambda=479$ nm), which disappears at pH 6.08 ($\lambda=531$ nm) due to full ground-state protonation of the dialkylanilines. Upon addition of aqueous KOH, no significant change in the absorption spectrum of **6** is observed. The small bathochromic shift in absorption is surprising and persists upon addition of excess KOH. Similar behavior is observed in the emission spectrum, with only a small $\lambda\approx20$ nm shift from $\lambda=529$ (pH 4.80) to 549 nm (pH 13.7). This band is distinct and does not change upon addition of excess KOH. It is not clear why only small bathochromic shifts are observed for **6** at high pH.

Interaction of hydroxydialkylamino XFs with metal salts: Figure 6 shows the absorbance and emission spectra of XFs **6** and **7** in the presence of different metal ions. Figure 7 displays photographs of both XFs before and after addition of an excess of ten different metal triflates. The experiments were conducted in MeCN and CH_2Cl_2. Although the addition of Mg^{2+}, Ca^{2+}, or Li^{+} does not lead to changes in fluorescence for **6**, the other metal cations produce changes in emission. For XF **7**, metal cations lead to either quenching or changes in emission color with the exception of Li^{+} in MeCN. The fluorescence changes are qualitatively similar to those observed upon protonation, but do not occur for each XF with every metal.

In MeCN, Zn^{2+}, Mn^{2+}, Sn^{2+}, Ba^{2+}, and Ag^{+} all result in a blueshift in the emission of **6**. The addition of Hg^{2+} quenches the emission of **6** due to a heavy atom effect, and paramagnetic Cu^{2+} is also an efficient quencher. Similar spectroscopic properties are observed in CH_2Cl_2, but Cu^{2+} induces a blueshift in the emission of **6**. The fluorescence changes are slightly different for **7** (Figure 6). In MeCN, Zn^{2+}, Mn^{2+}, Sn^{2+}, or Ba^{2+} result in a blueshift in emission, whereas the addition Mg^{2+}, Ca^{2+}, Hg^{2+}, and Cu^{2+} salts

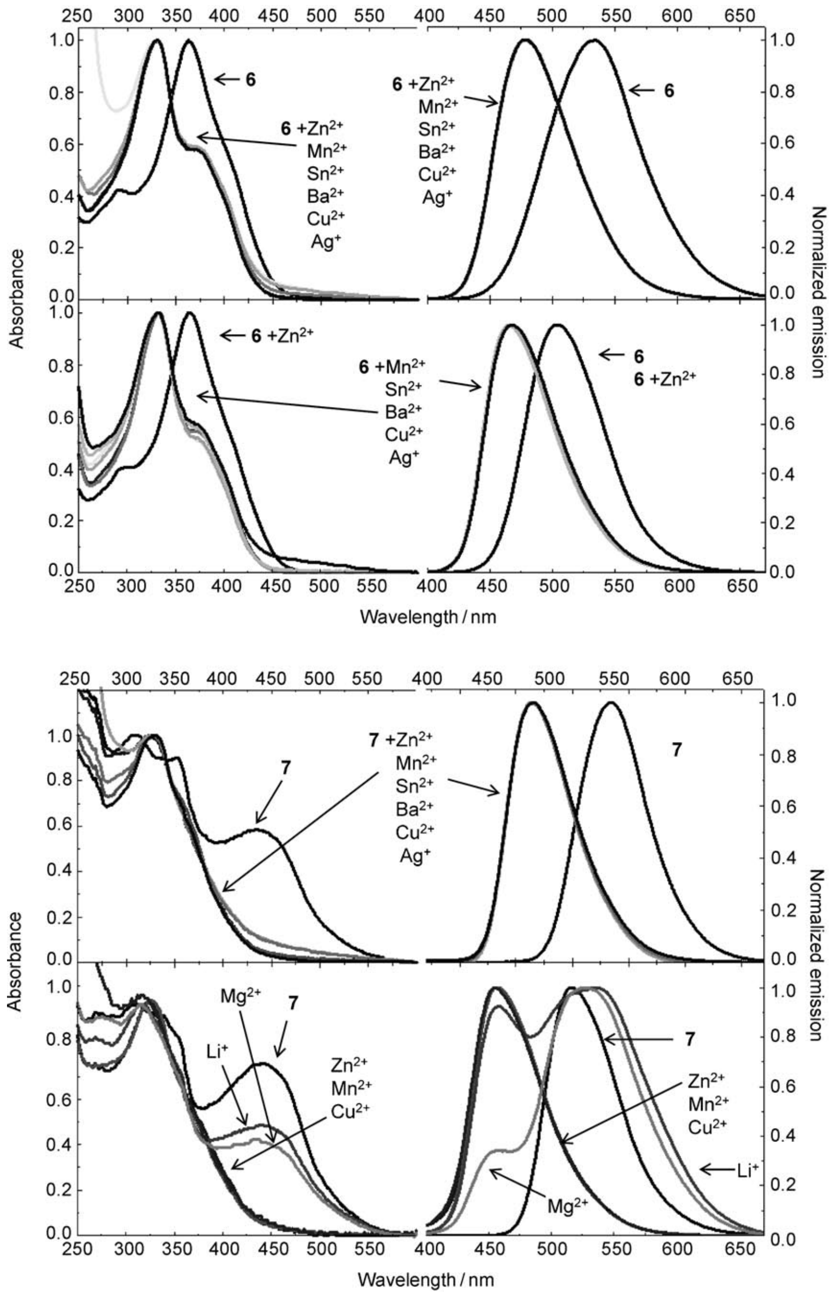

Figure 6. Normalized absorption (left) and emission (right) of **6** and **7** in MeCN (top) and CH_2Cl_2 (bottom) in the presence of different metal cations.

quench the fluorescence of **7**. In CH_2Cl_2, Zn^{2+}, Mn^{2+}, and Cu^{2+} are the only cations that result in blueshifts in the emission of **7**, whereas Mg^{2+} and Li^+ induce orange and yellow emissions, respectively. This is due to a dual emission that occurs between the complexed and uncomplexed forms of cations coordinated to the lone pairs of the dibutylanilines (see Figure 6).

Amine sensing with hydroxydialkylamino XFs: To observe the ability to utilize **6** as a potential amine sensor, a 10 μm stock solution of **6** was prepared in eight solvents and tested with ten different amines (0.1 mL per sample, 0.7–7.2 mm concentration range). Figure 8 shows real-color photographs of the amine-spiked samples upon UV illumination.

In the ground state, **6** forms weakly hydrogen-bonded complexes to the amines and the UV/Vis spectra of these samples do not show much change. The effect of the addition of amines upon the fluorescence of **6** can be dramatic and depends upon the amine–solvent combination. Emission colors of blue, green, yellow, or red are observed (Figure 8). Depending upon the solvent, we see proton transfer in various stages from a weak hydrogen-bonded complex to perhaps the formation of ion pairs (Figures 8 and 9).[18] If the amine under consideration is not very basic, such as morpholine and piperazine, there is little change in the fluorescence color and intensity, even though some changes are observed in the basic solvents DMF, DMSO, and acetonitrile. Putrescine, 1,3-diaminopropane, ethylenediamine, and DBU give the most distinct changes in fluorescence regardless of solvent. However, the pK_a of the ammonium ions is not the only determinant of a strong response, given that putresceine and piperazine have quite similar pK_a values (9.9 and 9.8, respectively) but display different responses.

The spectral data and photographs give some discrimination between the amines. We converted the color from the amine panel into RGB values and subtracted these from the reference (Contrast Analyzer).[19] This data was subjected to a linear discriminant analysis (LDA, program SYSTAT),[20] reducing the data into a 2D LDA plot that contains two factors by which all ten amines are separated (Figure 10). The plot shows the diamines grouped together in the top left corner, whereas the secondary amines, such as diethylamine and diisopropylamine, are grouped together in the bottom right corner.

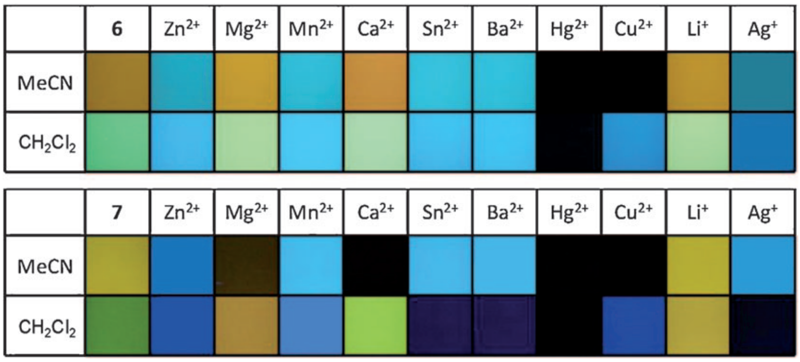

Figure 7. Exposure of **6** and **7** to different metal cations in MeCN and CH_2Cl_2. Photographs were taken under UV radiation at $\lambda_{em} = 366$ nm.

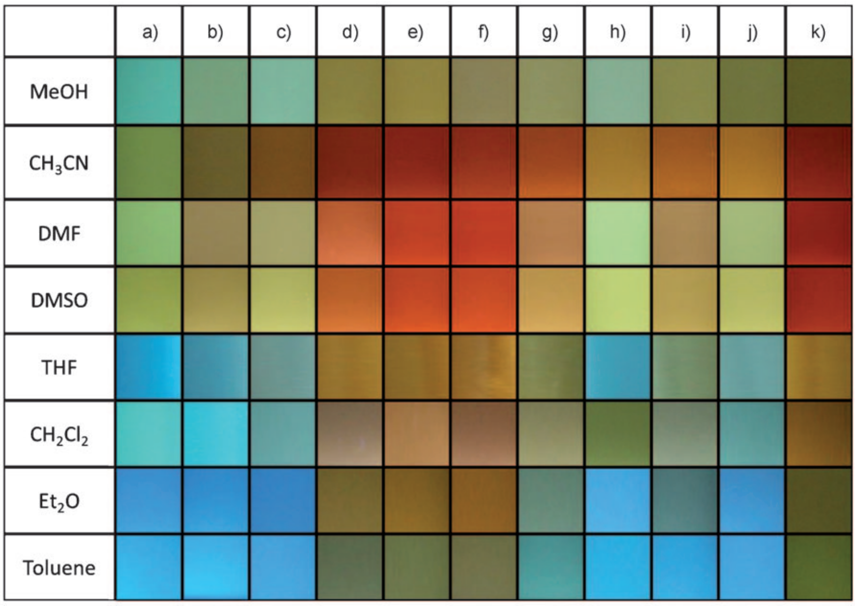

Figure 8. Exposure of **6** to different amines in various solvents. a) XF **6** only (reference), b) **6**+morpholine (8.33), c) **6**+piperazine (9.83), d) **6**+putrescine (9.90), e) **6**+1,3-diaminopropane (10.47), f) **6**+ethylenediamine (10.70), g) **6**+piperidine (10.80), h) **6**+triethylamine (10.80), i) **6**+diethylamine (11.00), j) **6**+diisopropylamine (11.10), k) **6**+1,8-diazabicyclo[5.4.0]undec-7-ene (DBU ~ 12). The numbers in parentheses are the pK_a values of the corresponding ammonium ions. Illumination was performed by using UV radiation at $\lambda_{em} =$ 366 nm.

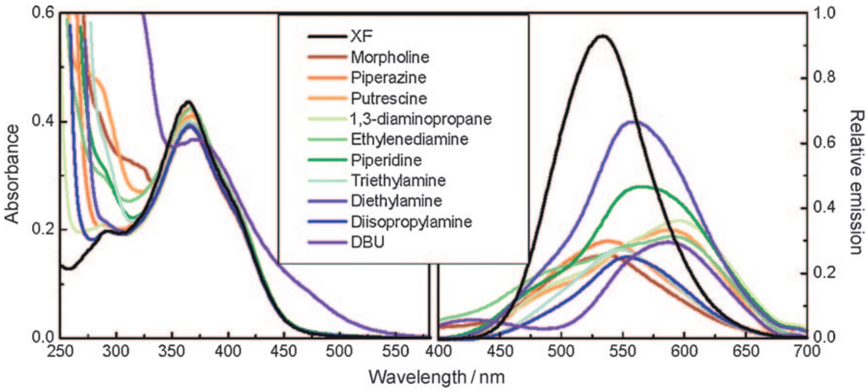

Figure 9. Absorption and emission of XF **6** on addition of different amines in MeCN.

Conclusion

We have prepared XFs **6** and **7**. XF **6** displays red- and blue-shifted absorption and emission upon protonation and deprotonation, whereas XF **7** displays similar properties, but its fluorescence is quenched in the presence of bases. Both XFs are cation-reactive, and **6** is a viable amine-reactive fluorophore that displays color shifts in different solvents. It would be useful to have amphoteric XF fluorophores, such as **6**, attached to polystyrene or glass beads. Exposure to acid or amine vapor would then lead to dramatic color changes, making these chromophores interesting as potential dosimeter-type amine-responsive materials. Such investigations are underway and will be reported elsewhere.

Experimental Section

The experimental details for the synthesis of XFs **6**, **7**, and their intermediates, and details of the photophysical experiments and the absorption and emission spectra for all systems studied are available in the Supporting Information.

Acknowledgements

We thank the National Science Foundation (CHE-0809179 for K.M.S. and L.M.T. and CHE-0750275 for U.B. and P.M.) and the Department of Energy (DE-FG02-04ER46141 for V.R. and O.M.) for generous financial support. P.M. thanks the Georgia Institute of Technology for a FACES fellowship. We thank Katya Kouznetsova for the frontispiece design.

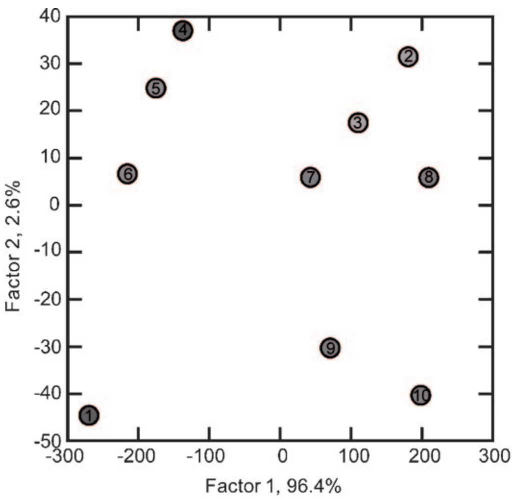

Figure 10. LDA analysis of the differential RGB values of **6** obtained from Figure 8; ①: DBU, ②: morpholine, ③: piperazine, ④: putrescine, ⑤: 1,3-diaminopropane, ⑥: ethylenediamine, ⑦: pipiridine, ⑧: triethylamine, ⑨: diethylamine, ⑩: diisopropylamine.

---

[1] A. J. Zucchero, P. L. McGrier, U. H. F. Bunz, *Acc. Chem. Res.* **2010**, *43*, 397–408.

[2] a) E. Bardez, *Isr. J. Chem.* **1999**, *39*, 319–332; b) S. Y. Park, D. J. Jang, *J. Am. Chem. Soc.* **2010**, *132*, 297–302.

[3] O. Poizat, E. Bardez, G. Buntinx, V. Alain, *J. Phys. Chem. A* **2004**, *108*, 1873–1880.

[4] K. M. Solntsev, O. Poizat, J. Dong, J. Rehault, Y. Lou, C. Burda, L. M. Tolbert, *J. Phys. Chem. B* **2008**, *112*, 2700–2711.

[5] a) J. A. Marsden, J. J. Miller, L. D. Shirtcliff, M. M. Haley, *J. Am. Chem. Soc.* **2005**, *127*, 2464–2476; b) J. A. Marsden, M. M. Haley, *J. Org. Chem.* **2005**, *70*, 10213–10226; c) J. A. Marsden, J. J. Miller, M. M. Haley, *Angew. Chem.* **2004**, *116*, 1726–1729; *Angew. Chem. Int. Ed.* **2004**, *43*, 1694–1697.

[6] a) A. Zen, A. Bilge, F. Galbrecht, R. Alle, K. Meerholz, J. Grenzer, D. Neher, U. Scherf, T. Farrell, *J. Am. Chem. Soc.* **2006**, *128*, 3914–3915; b) A. Bilge, A. Zen, M. Forster, H. B. Li, F. Galbrecht, B. S. Nehls, T. Farrell, D. Neher, U. Scherf, *J. Mater. Chem.* **2006**, *16*, 3177–3182.

[7] a) L. Gobbi, P. Seiler, F. Diederich, *Angew. Chem.* **1999**, *111*, 737–740; *Angew. Chem. Int. Ed.* **1999**, *38*, 674–678; b) F. Diederich, *Chem. Commun.* **2001**, 219–227; c) R. R. Tykwinski, U. Gübler, R. E. Martin, F. Diederich, C. Bosshard, P. Günter, *J. Phys. Chem. B* **1998**, *102*, 4451–4465; d) R. R. Tykwinski, M. Schreiber, R. P. Carlon, F. Diederich, V. Gramlich, *Helv. Chim. Acta* **1996**, *79*, 2249–2281; e) A. Hilger, J. P. Gisselbrecht, R. R. Tykwinski, C. Boudon, M. Schreiber, R. Martin, H. P. Lüthi, M. Gross, F. Diederich, *J. Am. Chem. Soc.* **1997**, *119*, 2069–2078; f) F. Mitzel, C. Boudon, J. P. Gisselbrecht, P. Seiler, M. Gross, F. Diederich, *Helv. Chim. Acta* **2004**, *87*, 1130–1157; g) J. P. Gisselbrecht, N. N. P. Moonen, C. Boudon, M. B. Nielsen, F. Diederich, M. Gross, *Eur. J. Org. Chem.* **2004**, 2959–2972.

[8] Z. I. Niazimbetova, H. Y. Christian, Y. J. Bhandari, F. L. Beyer, M. E. Galvin, *J. Phys. Chem. B* **2004**, *108*, 8673–8681.

[9] A. J. Zucchero, J. N. Wilson, U. H. F. Bunz, *J. Am. Chem. Soc.* **2006**, *128*, 11872–11881.

[10] a) P. L. McGrier, K. M. Solntsev, J. Schönhaber, S. M. Brombosz, L. M. Tolbert, U. H. F. Bunz, *Chem. Commun.* **2007**, 2127–2129; b) P. L. McGrier, K. M. Solntsev, S. Miao, L. M. Tolbert, O. R. Miranda, V. M. Rotello, U. H. F. Bunz, *Chem. Eur. J.* **2008**, *14*, 4503–4510.

[11] L. Horner, H. Hoffman, H. G. Wippel, G. Klahre, *Chem. Ber.* **1959**, *92*, 2499–2505.

[12] a) K. Sonogashira, *J. Organomet. Chem.* **2002**, *653*, 46–49; b) U. H. F. Bunz, *Chem. Rev.* **2000**, *100*, 1605–1645.

[13] a) M. J. Kamlet, J. L. M. Abboud, M. H. Abraham, R. W. Taft, *J. Org. Chem.* **1983**, *48*, 2877–2887; b) Y. Wu, P. V. Lawson, M. M. Henary, K. Schmidt, J.-L. Bredas, C. J. Fahrni, *J. Phys. Chem. A* **2007**, *111*, 4584–4595.

[14] a) K. M. Solntsev, D. Huppert, L. M. Tolbert, N. Agmon, *J. Am. Chem. Soc.* **1998**, *120*, 7981–7982; b) K. M. Solntsev, D. Huppert, N. Agmon, *J. Phys. Chem. A* **1998**, *102*, 9599–9606; c) J. Dong, K. M. Solntsev, L. M. Tolbert, *J. Am. Chem. Soc.* **2006**, *128*, 12038–12039.

[15] a) D. Z. Mijin, G. S. Uscumlic, N. U. Perisic-Janjic, N. V. Valentic, *Chem. Phys. Lett.* **2006**, *418*, 223–229; b) M. Reta, R. Cattana, J. J. Silber, *J. Solution Chem.* **2001**, *30*, 237–252; c) B. Z. Magnes, D. Pines, N. Strashnikova, E. Pines, *Solid State Ionics* **2004**, *168*, 225–233.

[16] S. M. Brombosz, A. J. Zucchero, P. L. McGrier, U. H. F. Bunz, *J. Org. Chem.* **2009**, *74*, 8909–8913.

[17] A. J. Zucchero, J. Tolosa, L. M. Tolbert, U. H. F. Bunz, *Chem. Eur. J.* **2009**, *15*, 13075–13081.

[18] a) F. D. Lewis, E. M. Crompton, *J. Am. Chem. Soc.* **2003**, *125*, 4044–4045; b) F. D. Lewis, L. E. Sinks, W. Weigel, M. C. Sajimon, E. M. Crompton, *J. Phys. Chem. A* **2005**, *109*, 2443–2451; c) L. M. Tolbert, K. M. Solntsev, *Acc. Chem. Res.* **2002**, *35*, 19–27; d) K. M. Solntsev, P. L. McGrier, C. J. Fahrni, L. M. Tolbert, U. H. F. Bunz, *Org. Lett.* **2008**, *10*, 2429–2432.

[19] The Contrast Colour Analyzer program is freeware and can be downloaded from http://www.visionaustralia.org.au/info.aspx?page=1985.

[20] a) R. G. Brereton, *Chemometrics: Data Analysis for the Laboratory and Chemical Plant*, Wiley, New York, **2003**; b) K. J. Albert, N. S. Lewis, C. L. Schauer, G. A. Sotzing, S. E. Stitzel, T. P. Vaid, D. R. Walt, *Chem. Rev.* **2000**, *100*, 2595–2626.

Received: October 5, 2010